Max-Planck-Institut für Meteorologie

REPORT No. 238

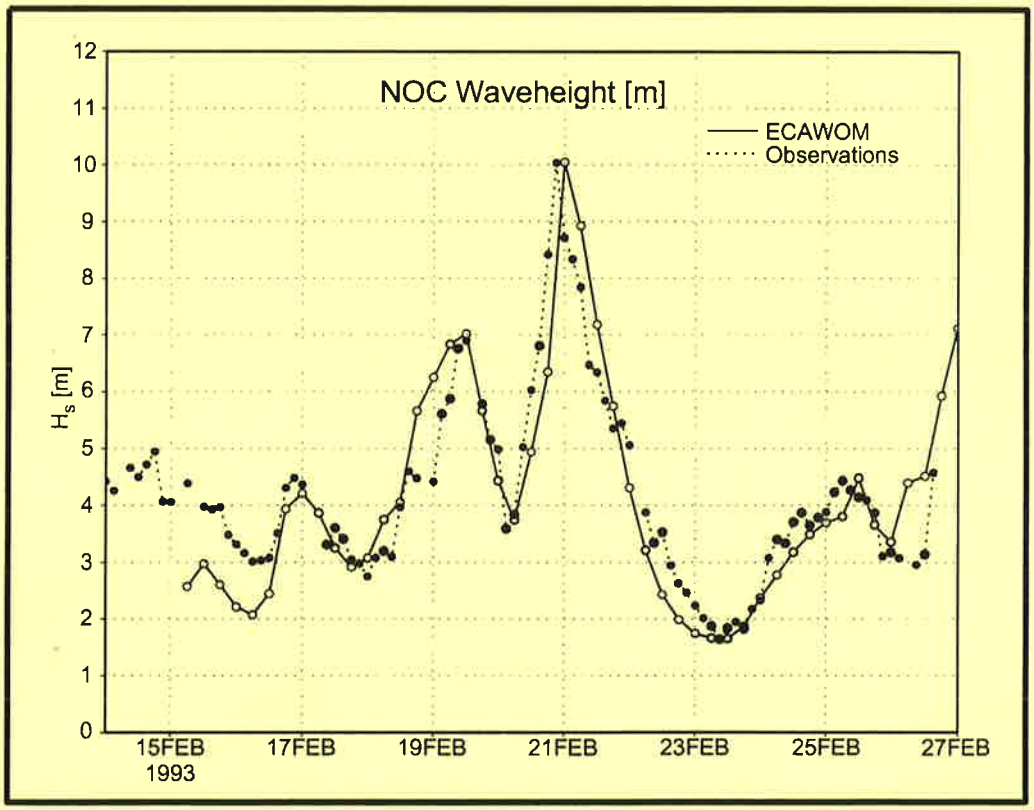

THE EUROPEAN COUPLED ATMOSPHERE WAVE OCEAN MODEL ECAWOM

by

Ralf Weisse · Enrique F. Alvarez

HAMBURG, July 1997

AUTHORS:

Ralf Weisse

GKSS Institut für Gewässerphysik
Max-Planck-Str. 1
D-21502 Geesthacht
Germany

Enrique F. Alvarez

Clima Maritimo
Puertos del Estado-CEDEX
Antonio Lopez 81
E-28026 Madrid
Spain

MAX-PLANCK-INSTITUT
FÜR METEOROLOGIE
BUNDESSTRASSE 55
D - 20146 HAMBURG
GERMANY

Tel.: +49-(0)40-4 11 73-0
Telefax: +49-(0)40-4 11 73-298
E-Mail: <name> @ dkrz.de

The European Coupled Atmosphere Wave Ocean Model ECAWOM

Ralf Weisse

Max-Planck-Institut für Meteorologie, Hamburg, Germany

(present affiliation: GKSS Research Centre, Geesthacht, Germany)

Enrique F. Alvarez

Programa de Clima Marítimo (Puertos del Estado), Madrid, Spain

ISSN 0937 - 1060

Correspondence: weisse@gkss.de

Abstract

The European Coupled Atmosphere Wave Ocean model ECAWOM and its application to a North Sea storm are described. The model was integrated for the 1 month period of February 1993. Preliminary analysis of the results suggest that the model is capable of reproducing the basic features of the atmospheric, the wave, and the surge characteristics for this 1 month period. However, further analysis and integrations are needed to fully assess the skill of the developed model, its potential for long term integrations, and the impact of sea state dependent air-sea fluxes on the atmospheric and the oceanic circulation.

1. Introduction

The dynamical evolution of the atmospheric and the oceanic circulation is strongly influenced by the presence of property fluxes at the air-sea interface such as the momentum flux, the heat flux, or the freshwater flux. Several studies show that these fluxes are sea state dependent (e.g. Janssen, 1989, 1991, Chalikov and Makin, 1991, Makin, 1996). Especially the impact of waves on the momentum transfer at the sea surface was studied intensively in recent years although opinions about the significance of the effects on the atmospheric circulation differ (e.g. Weber, 1994, Janssen and Viterbo, 1996). It is, however, generally agreed that there is an increasing effect of waves on the momentum flux from larger to smaller spatial scales.

Another way in which the ocean circulation may be influenced by the presence of waves is known as wave-current interaction. A wind event which causes surface gravity waves would also generate a storm surge and vice versa. Their generation is thus closely related and there are several known mechanisms by means of which the mean flow or the water level associated with tide and surge and the waves can interact. In very shallow water, where the prediction of waves, surges, and tides is essential for coastal protection, the influence of these interactions may be substantial (e.g. Wolf et al., 1988). Presently there exists a number of highly sophisticated coupled wave-ocean models which account for these effects (e.g. Flather et al., 1991). However, the region which is usually covered by these models is much smaller than the scale on which global or nearly global models are considered to be skilful (“skilful scale”). The skilful scale is typically on the order of a few grid points (von Storch, 1995). It is thus impossible to drive small-scale models directly with boundary conditions obtained from large-scale (global) models. Additionally the large-scale models are often uncoupled, so that assumptions for the lateral boundaries of the other model components have to be made.

The limited area coupled atmosphere-wave-ocean model (ECAWOM - European Coupled Atmosphere Wave Ocean Model) was developed and set-up to derive user-oriented scale information from large-scale boundaries, simultaneously for the atmosphere, the wave field, and the ocean. In this sense, the model fits into the dynamic downscaling approach (Giorgi and Mearns, 1991), in which higher-resolution numerical models are nested into coarser-resolution models or are driven by boundary information obtained from the large-scale model. Since high-resolution limited area models contain high-resolution information, e.g. about the regional topography, they are able to simulate the regional circulation much more faithfully.

The chain of numerical weather forecast models used by national weather services can be seen from the view of dynamical downscaling, similarly as the so-called time-slice experiments, in which high-resolution atmosphere models are forced by boundary conditions simulated in a low-resolution model. With ECAWOM dynamical downscaling is applied simultaneously to the atmosphere, the waves, and the ocean.

It is the objective of ECAWOM to fill the gap between the large-scale uncoupled atmosphere and the small-scale wave-ocean models. ECAWOM is thus designed to operate on horizontal grids of tens of kilometres and to cover regions of some 1000 km, much larger than the skilful scale of global or nearly global models. The output of ECAWOM is a consistent simultaneous data set for the atmosphere, the waves and the ocean which can be used directly by the small-scale models. Therefore, ECAWOM does not include all physical processes which are modified by the presence of waves, but only those which are important on the ECAWOM scale.

ECAWOM as it now exists is in a preliminary state and only a very limited number of tests were performed so far. Further analysis and tests are needed to fully assess the skill of the developed model and its potential for long term integrations. The purpose of the present paper is to briefly describe the ECAWOM model and the results of a 1 month hindcast of a stormy period over the North Sea in February 1993. The paper is organized as follows. In Section 2 the model and the physics of the processes at the air- sea interface are described. Technical aspects such as exchange of information or boundary conditions are briefly discussed in Section 3. In Section 4 we present first results of the analysis of the application of ECAWOM to the North Sea storms of February 1993. In Section 5 the results are summarized and future plans are presented.

2. Concept of ECAWOM

2.1. Short description of ECAWOM modules

As a coupled atmosphere-wave-ocean model, ECAWOM consists of three independent models, namely an atmosphere model, a wave model, and an ocean model. We hereafter refer to these models as modules. The coupling interface is also denoted as a module, and contains the physics of the air-sea interaction and partially those of the wave-current interaction. We also use the terminology “module” to refer to different physics packages available for the atmosphere model.

ECAWOM is programmed in a modular structure with the objective of making the replacement or addition of modules as easy as possible. The principal layout can be inferred from Figure 1. There are the two alternative atmosphere modules HIRLAM and HIRHAM, the

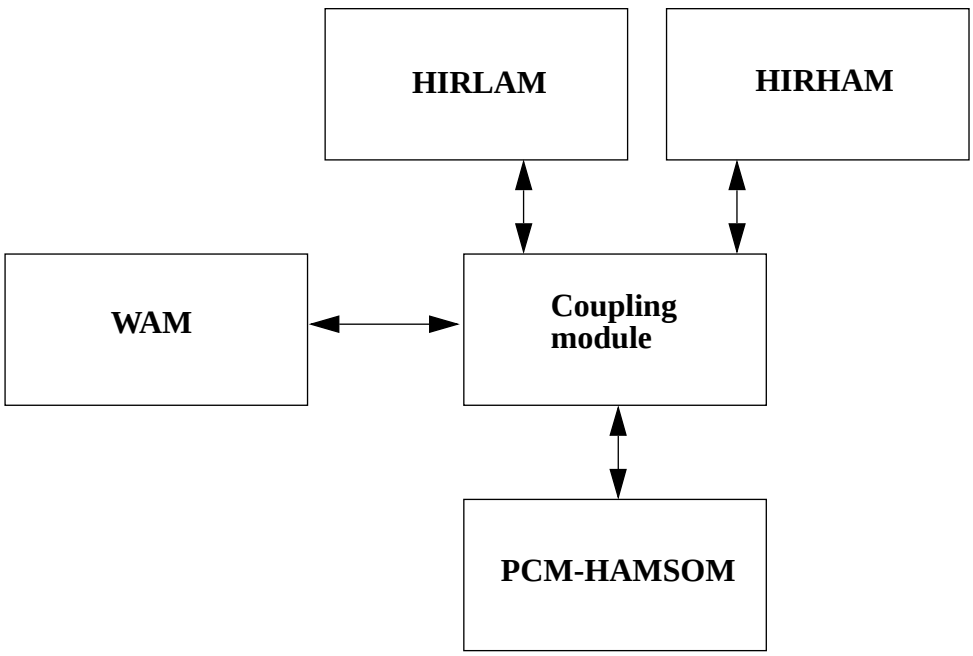

Figure 1: Sketch of the ECAWOM principal structure.

wave module WAM, and the ocean module PCM-HAMSOM. They are connected via a coupling module which is responsible for the transformation, the re-scaling, and the exchange of information among the atmosphere, the waves, and the ocean.

2.1.1. The HIRLAM and HIRHAM modules

The HIgh Resolution Limited Area Model (HIRLAM) is used as the atmospheric module in ECAWOM. We used the version of the Max-Planck-Institut für Meteorologie in Hamburg (MPIfM) which additionally includes a more sophisticated physics package (HIRHAM, HIgh Resolution limited-area model with HAMburg physics package). This package was especially designed for long-term climate integrations. It is identical to that used in the global general circulation model ECHAM (DKRZ Modelling Group, 1993). The HIRLAM and the HIRHAM physics can be used alternatively. However, tests were performed only for the HIRLAM module, and coupling of the numerically more expensive HIRHAM module has not yet been completed.

The HIRLAM forecasting system is a limited-area, primitive equation model which uses a grid-point representation with second-order difference approximations for the spatial derivatives. It was designed as a short-range weather forecasting system and is based on the hydrostatic approximation. The prognostic variables are horizontal wind, temperature, specific humidity, and surface pressure. Over land, surface temperature, surface wetness, and snow depth are also predicted.

Horizontally HIRLAM is formulated on an ARAKAWA C-grid (Arakawa and Lamb, 1977) in a rotated spherical coordinate system. The vertical coordinate is a general terrain-following hybrid coordinate, which near the surface is pressure normalized by surface pressure (σ), and approaches pressure with increasing height (Simmons and Burridge, 1981).

The forecasting system was originally developed as a cooperative project between several European meteorological institutes. As a limited-area model the HIRLAM system is intended for use with lateral boundary conditions from a global model such as the ECMWF forecasting system. It is also possible to run a sequence of HIRLAM systems nested within one other, but informations are transferred only from the larger to the smaller area. Details on the model physics and dynamics can be found in Källén (1996).

The HIRHAM limited-area model was developed from the HIRLAM system in order to facilitate long-term climate runs with boundaries from the ECHAM (DKRZ Modelling Group, 1993) global climate model. Thus the HIRLAM physics package has been replaced by that of the ECHAM3 model (Christensen and Maijgaard, 1992). A detailed description of the adiabatic part of HIRHAM can be found in the HIRLAM documentation manual (Källén, 1996)

and that of the physical parameterizations in the DKRZ ECHAM3 documentation manual (DKRZ Modelling Group, 1993).

2.1.2. The WAM module

In ECAWOM we use the third generation wave model WAM (WAMDI, 1988) to calculate the wave state. In contrast to first and second generation models, the third generation model WAM introduces no ad hoc assumptions on the spectral shape. The WAM model describes the evolution of a two-dimensional ocean wave spectrum and computes the 2-d wave variance spectrum through integration of the transport equation

$$\frac{\partial}{\partial t}F(f,\Theta) + \nabla\bullet(c_g F(f,\Theta)) = S_{in} + S_{dis} + S_{bot} + S_{nl} \qquad (1)$$

where $F(f,\Theta)$ is the wave spectrum, f the frequency and Θ the direction of a wave component. $c_g = \frac{\partial\omega}{\partial k}$ is the group velocity with $\omega = 2\pi f$. The terms on the right hand side of (1) denote the source functions. They represent the wind input (S_{in}), the dissipation due to whitecapping (S_{dis}), the bottom dissipation (S_{bot}), and the non-linear wave-wave interaction (S_{nl}).

The wind input term was adopted from Snyder et al. (1981) with a scaling with friction velocity u_*. Wind input and dissipation terms of the present cycle are a further development based on Janssen's quasi-linear theory of wind-wave generation (Janssen, 1989, 1991).

The sea surface waves extract momentum from the air flow, therefore, the stress in the surface layer depends both on the wind speed and the wave-induced stress τ_w. The growth rate γ of the waves is then determined by the friction velocity u_* and the roughness length z_0.

The wind input term is given by

$$S_{in} = \gamma F \qquad (2)$$

For a logarithmic wind profile, γ depends only on two parameters (Miles, 1957), namely

$$X = u_* \cos(\Theta - \Phi) C^{-1} \qquad (3)$$

$$\Omega = \frac{gz_0}{u_*} \tag{4}$$

where u_* is the friction velocity, Θ the direction in which the waves propagate, Φ the wind direction, C the phase speed of the waves and z_0 the roughness length. Thus, through Ω the growth rate depends on the roughness, which in turn depends on the sea state. The growth rate, normalized by angular frequency ω, is given by

$$\frac{\gamma}{\omega} = \varepsilon\frac{\beta_m}{\kappa^2}\mu(\ln\mu)^4 X^2, \mu < 1 \tag{5}$$

with κ the van Carman constant, $\beta_m = 1.2$ a constant and $\mu = kz_c$ is the dimensionless critical height with k the wave number and z_c the critical height defined by $U_0(z = z_c) = C$.

The roughness z_c and the friction velocity follow from the theory of Janssen (1991) which is briefly described in Section 2.1.4.1. In this theory the wave-induced stress τ_w is required. It follows from the conservation of momentum by

$$\hat{\tau}_w = \rho_w \int_0^{\infty}\int_0^{2\pi} S_{in}(f,\theta)\frac{\hat{k}}{k}\omega d\Theta df \tag{6}$$

and closes the set of equations. For details we refer to the WAM manual (Günther et al., 1992) and to the Section 2.1.4.1. of the present paper. A comprehensive description may be found in Komen et al. (1994) or in WAMDI (1988).

2.1.3. The PCM-HAMSOM module

The HAMburg Shelf Ocean Model (HAMSOM) in the version of Programa de Clima Marítimo (PCM-HAMSOM) is used as the ocean model in ECAWOM. PCM-HAMSOM is a three-dimensional baroclinic primitive equation model. The basic frame is the model described in Backhaus (1983) and Backhaus (1985). It was further developed by PCM, and within ECAWOM we use the version described by Alvarez (1995).

The prognostic variables are the horizontal velocity components, temperature, salinity and sea surface elevation. A number of quantities are derived diagnostically. The hydrostatic approximation is applied, balancing the vertical pressure gradient and the acceleration of gravity. Water is treated as an incompressible fluid. The Boussinesq approximation is taken; it states that if changes in density are small, they will be considered only in the buoyancy term and will

be neglected elsewhere.

The model uses finite differences to compute the spatial gradients. A semi-implicit scheme is used to compute the time derivatives at a number of layers. The model may be run either in a barotropic or in a full baroclinic mode, taking temperature and salinity changes and their advection into account.

The UNESCO (1983) formulae is used to compute the density. The model is formulated on an ARAKAWA C-grid in cartesian coordinates. For the purposes of ECAWOM it was transformed to rotated spherical coordinates.

A number of options exist to apply different parameterizations for a number of processes, such as e.g. the Richardson scheme or the Kochergin scheme for turbulent eddy viscosity. Details about the HAMSOM model can be found for instance in Backhaus (1983, 1985), Alvarez (1995), or Rodriguez (1996). A very detailed description of the numerics is given in Huang (1995).

2.1.4. The Coupling module

The presence of waves modifies the fluxes at the air-sea interface, such as the momentum flux, the heat flux, the moisture flux, the flux of CO_2, etc. Furthermore, there is interaction among waves, surges, currents and tides.

For an overview and a detailed description of these processes we refer to Wolf et al. (1988) and to Mastenbroek and Christopoulos (1995). In this paper we will denote only those processes which are relevant at ECAWOM scales and which were introduced into the coupling module. These processes are discussed in detail in the following section.

2.1.4.1. The momentum flux

The momentum flux was parameterized according to Janssen (1989, 1991). If we neglect the impact of viscosity and assume the wind to be constant in time and space, the momentum balance equation reduces to

$$\frac{\partial \tau}{\partial z} = 0 \qquad (7)$$

where τ denotes the total momentum flux and z the vertical coordinate. The total momentum

flux can be broken into a turbulent part τ_t and a wave-induced part τ_w

$$\tau = \tau_t + \tau_w \tag{8}$$

The turbulent part of the stress is usually parameterized by means of a mixing length hypothesis

$$\tau_t = \rho_a (\kappa l)^2 \left(\frac{\partial U}{\partial z}\right)^2 \tag{9}$$

where ρ_a is the density of air, $\kappa = 0.4$ the van Carman constant and $U(z)$ the wind speed at height z.

Wave-independent stress. The wave-induced part of the stress is usually neglected when coupling atmosphere and ocean models, and it is assumed that the ocean gains all momentum lost by the atmosphere. Since the ocean receives momentum at much lower (current) speeds than is provided by the atmosphere, the waves gain energy, but no momentum. Neglecting the wave-induced stress in (8), integration of (7) by means of (9) yields

$$U(z) = \frac{u_*}{\kappa} \ln\left(\frac{z}{z_0}\right) \tag{10}$$

which is known as the logarithmic wind profile. $u_* = (\tau \rho_a^{-1})^{0.5}$ is the so-called friction velocity, and the integration constant z_0, known as the roughness length, is usually parameterized by

$$z_0 = \frac{\alpha u_*^2}{g} \tag{11}$$

Equation (11) is called the Charnock relation and was derived by Charnock (1955) on dimensional reasons. If the Charnock parameter α is given, an implicit relation between wind stress and wind speed at a certain height is found. In that case, the drag coefficient C_D is fully determined by the roughness length

$$C_D(z) = \left(\frac{u_*}{U(z)}\right)^2 = \left(\frac{\kappa}{\ln\left(\frac{z}{z_0}\right)}\right)^2 \tag{12}$$

Wave-dependent stress. There exist different consistent theories of wind-wave coupling (e.g. Chalikov and Makin (1991) and Makin (1995) or Janssen (1989, 1991)). Here we will discuss only the theory of Janssen (1989, 1991), which was incorporated into ECWAOM.

Janssen (1991) assumes that the velocity profile is modified by the presence of waves so that the wind speed U at height z can be written as

$$U(z) = \frac{u_*}{\kappa} \ln\left(\frac{z + z_e - z_0}{z_e}\right) \tag{13}$$

It can be shown that, if this velocity profile holds true, the effective roughness z_e is given by

$$z_e = \frac{z_0}{\sqrt{1 - \tau_w \tau^{-1}}} \tag{14}$$

For the roughness length z_0, Janssen assumes a background Charnock relation to be valid

$$z_0 = \frac{\tilde{\alpha} u_*^2}{g} \tag{15}$$

and the background Charnock parameter $\tilde{\alpha}$ is tuned such that $z_e = z_0$ for old wind sea. Thus, the wind stress is enhanced in Janssen's model if $\tau_w \tau^{-1}$ approaches one, but behaves according to Charnock if $\tau_w \tau^{-1}$ is small.

In ECAWOM equations (14) and (15) are used to compute the drag coefficient (12). To take the stability of the atmospheric boundary layer into account, the drag is further modified by analytical functions f depending on the Richardson number Ri. These functions were proposed by Louis (1979) and Louis et al. (1982), and are part of the HIRLAM physics package. For details see Källén (1996).

2.1.4.2. The energy budget at the sea surface

The energy budget of the first ocean layer can be written as

$$c_p \rho \frac{dT}{dt} = Q_{rad}^{sfc} - Q_{sh} - Q_{lh} - Q_g - Q_m \tag{16}$$

where c_p denotes the specific heat at constant pressure, ρ the density, and T the temperature of the first ocean layer. Q_{rad}^{sfc} is the net flux of radiation at the surface, Q_{sh} the (direct) sensible

heat flux which results from the difference in the temperature of the sea surface and the overlying air, Q_{lh} the (indirect) latent heat flux which results mainly from evaporation at the sea surface and later condensation within the atmosphere, Q_g the flux of energy into the subsurface mainly due to heat conduction, and Q_m the energy used for snow and ice melt at the rate M_s and for freezing of water at the rate F_s

$$F_m = l_m(M_s - F_s) \tag{17}$$

where l_m represents the heat of melt.

The term Q_g is part of the ocean module and does not need to be considered in the coupling module. Since sea ice is so far given by climatology, we also do not consider the term Q_m and neglect the contribution which might arise from the fact that ocean temperatures drop below the freezing point. The term Q_{rad}^{sfc}, the sum of incoming and outgoing, short- and longwave radiation at a box at the sea surface, can be represented as

$$Q_{rad}^{sfc} = Q_{rad}^{sfc}(T_S, X_a) \tag{18}$$

where T_S denotes the sea surface temperature, and X_a the dependency of Q_{rad}^{sfc} on a number of atmospheric parameters, such as the radiation balance of the box above, the cloud cover, etc. From (18) it can be inferred that the only non-atmospheric variable Q_{rad}^{sfc} depends on is the sea surface temperature. In ECAWOM we use the sophisticated radiation scheme of HIRLAM to compute the radiation term. However, instead of the climatological T_S, we use the T_S forecast by the ocean module to compute the radiation term.

Wave-independent case. Usually bulk formulas are applied to relate the sensible heat flux Q_{sh} and the latent heat flux Q_{lh} to the measured variables at the surface and at a certain height:

$$\frac{Q_{sh}}{\rho_a c_p} = C_{sh}(s_z - s_s)(U_z - U_s) \tag{19}$$

$$\frac{Q_{lh}}{\rho_a l_v} = C_{lh}(q_z - q_s)(U_z - U_s) \tag{20}$$

Here C_{sh} and C_{lh} are the exchange coefficients for sensible and latent heat respectively, analog to the drag coefficient in the parameterization of the momentum flux. U is the wind speed, $s = c_p T + gz$ is the dry static energy, q is the specific humidity, and l_v denotes the specific latent heat of evaporation. The subscripts z and s denote the values at height and at the surface. The surface drift velocity U_s is usually ignored.

By analogy with the derivation made in the previous section C_{sh} and C_{lh} can be expressed in terms of "roughness lengths" z_{ot} and z_{oq}, respectively

$$C_{sh}(z) = \sqrt{C_D}\kappa\left[\ln\left(\frac{z}{z_{0t}}\right)\right]^{-1} \tag{21}$$

$$C_{lh}(z) = \sqrt{C_D}\kappa\left[\ln\left(\frac{z}{z_{0q}}\right)\right]^{-1} \tag{22}$$

Thus the profiles yield

$$s(z) = \frac{s_*}{\kappa}\ln\left(\frac{z}{z_{0t}}\right) \tag{23}$$

$$q(z) = \frac{q_*}{\kappa}\ln\left(\frac{z}{z_{0q}}\right) \tag{24}$$

where s_* and q_* denote the equivalent to the friction velocity, i.e flux normalized by density.

Wave-dependent case. Measurements of sensible and latent heat flux give clear indications that the exchange coefficients for heat and moisture are much less dependent on wind speed and the sea state than is the drag coefficient (e.g. Makin, 1996). There is, however, a large scatter within the data which obscures the actual dependencies. The most common parameterization is to assign a constant value to the exchange coefficients (e.g. Pond et al., 1971, Smith, 1980, Smith, 1988, Large and Pond, 1982). Large and Pond (1982) argued that a constant z_{0t} would be more appropriate than a constant C_{sh} parameterization, although the statistical improvement of the fit to the data was not significant. From (21) it immediately follows, however, that such a choice does make a difference compared to the constant C_{sh} parameteriza-

tion. Since C_{sh} is proportional to the square root of the drag coefficient, C_{sh} would increase by as much as 50% for high wind speeds compared with the constant C_{sh} parameterization.

Makin (1996) extensively reviewed experimental parameterizations and, because of these limitations in the data sets, established a simple model to establish theoretical dependence of the exchange coefficients on wind speed. He found that for the exchange of sensible heat at the sea surface, there is no counterpart to the effective exchange mechanisms for momentum due to the form drag. Momentum is to a large extent transported by the organized wave-induced motions correlated with the waves, the form drag. Heat is transported only by viscosity. Makin (1996) computed the exchange coefficients for heat from the wind speed and the sea state using an approach which is based on the conservation of momentum and energy in the turbulent boundary layer above sea waves. He found that C_{sh} is virtually independent of wind speed for winds between 3 and 10 m/s. For winds within 10 to 20 m/s C_{sh} increased by roughly 10%, which is less than is estimated by the constant z_{0t} parameterization. He concluded that his theory favours the constant C_{sh} parameterization rather than the constant roughness. For practical purposes, Makin recommended for neutrally stable conditions

$$10^3 C_{sh} = 0.029\sqrt{C_D} \tag{25}$$

$$C_{lh} = 1.2 C_{sh} \tag{26}$$

In ECAWOM we used the standard HIRLAM formulation to compute the exchange coefficients for sensible and latent heat, and thus the related part of the heat fluxes. The sea state dependence enters these equations via the dependence of the drag on the sea state. The exchange coefficients are modified by analytical functions of the Richardson number as proposed by Louis (1979) and Louis et al. (1982) to account for the dependence of the exchange coefficients on the stability of the atmospheric boundary layer. For details see Källén (1996).

2.1.4.3. The freshwater flux

So far the freshwater flux coupling has been implemented only rather sloppily. Since our main goal was to run the model for periods of some weeks up to a month, we assumed that a good representation of the freshwater flux is not crucial at these scales. Precipitation and evaporation in the atmosphere module are determined as described in Källén (1996). The freshwater

fluxes necessary as boundary conditions for the sea surface salinities are computed by simply restoring to the sea surface salinities of Levitus (1982) which were used to initialize the ocean module. This kind of boundary condition is often used in long-term integrations of stand-alone ocean models. We are, however, aware of the fact that this representation of the freshwater flux is inconsistent and should not be applied for long-term integrations.

2.1.4.4. Other interactions among the modules

Sea surface pressure. Sea surface pressure computed by the atmosphere module is passed to the ocean module to take into account the inverse barometric effect.

Wave-current interaction. A horizontal shear of currents may cause wave refraction. The rate of change of wave direction Θ due to current gradients can be expressed by (Komen et al., 1994)

$$\frac{d\Theta}{dt} = \frac{1}{R}\left(\sin\Theta\left[\cos\Theta\frac{\partial u_\phi}{\partial\Phi} + \sin\Theta\frac{\partial u_\lambda}{\partial\Phi}\right] - \frac{\cos\Theta}{\cos\Phi}\left[\cos\Theta\frac{\partial u_\phi}{\partial\lambda} + \sin\Theta\frac{\partial u_\lambda}{\partial\lambda}\right]\right) \qquad (27)$$

Here R is the radius of the earth, and u is the current velocity. The subscripts Φ and λ denote latitude and longitude, respectively.

If we consider waves propagating parallel to the north $(\Theta = 0)$, equation (27) yields

$$\frac{d\Theta}{dt} = -\frac{1}{R\cos\Phi}\frac{\partial u_\phi}{\partial\lambda} \qquad (28)$$

If we suppose a northward current, decreasing in magnitude from the west to the east, the change of wave direction in (28) becomes positive, indicating that waves will turn to the right. The most dramatic effect occurs when waves are travelling against the currents. For sufficiently large currents, wave propagation is prohibited and reflection occurs.

In ECAWOM the standard formalism of WAM is used to compute the current refraction of waves. For details we refer to the WAM manual (Günther et al., 1992). In contrast to WAM, in which constant current velocities are assumed and the refraction terms are computed in a preprocessing step, ECAWOM re-computes the refraction terms after each ocean time step, when new current velocities are available assuming slowly varying conditions with respect to the time scale (wave period) and the space scale (wavelength). For the coupling we used the current velocities of the uppermost ocean layer. Effects which are due to vertical gradients of the

currents are neglected so far.

3. Some technical aspects of ECAWOM

ECAWOM operates on rotated spherical coordinates. HIRLAM and PCM-HAMSOM are formulated on an Arakawa C-grid. The wave model is formulated on a non-staggered grid. The location of the grid points in WAM is identical with the location of the scalar points in HIRLAM and PCM-HAMSOM.

As a limited-area model ECAWOM needs to be supplied with two types of boundary files, such general files as topography, albedo, soil-moisture, initial temperature and salinity for the ocean, etc., and lateral boundary conditions varying over time for the atmosphere, the wave and the ocean module. We hence will refer to the first type of boundary files as climate files. A set of routines is available to set-up the necessary climate files for the ECAWOM grid. Note, that so far sea ice is also given by climatology, i.e. its distribution is contained in the climate file and can be updated once a month at maximum. To do so, WAM has to be re-initialized.

For the time-dependent boundary files several options exist. They are briefly described below.

Lateral boundaries for HIRLAM. A simplified Davis relaxation technique (Kållberg and Gibson, 1977) is used to relax the model's dependent variables at $t + \Delta t$ towards externally specified time-dependent values within a narrow boundary relaxation zone. The model value x_i is set to x_{ni} at each grid point i by

$$x_{ni} = \alpha_i x_{Bi} + (1 - \alpha_i) x_i \,, \tag{29}$$

where x_{Bi} are the prescribed time-dependent boundary values. The non-zero weights α_i decrease from almost one at the boundary to almost zero within a narrow (typically 8 grid points) relaxation zone. HIRLAM includes powerful interpolation routines (Källén, 1996) so that the input does not necessarily have to be on the same grid. So far there are interfaces available to force HIRLAM with ECMWF forecasts or analyses or output from the global MPIfM climate model ECHAM.

Lateral boundaries for WAM. There are three options available. The first is simply to close the basin. For some applications, such as for the Baltic Sea or for the Mediterranean Sea, this

might provide a reasonable approximation. Option two is a simple continuation of the spectrum at the boundaries. We set the boundary value of the spectrum to 90% of its inner point.

$$F_{Boundary} = 0.9 F_{Boundary-1} \tag{30}$$

In this way an artificial fetch is created. This kind of boundary condition was proposed by Burgers (1990) and is used in the wave forecasting system of KNMI (Koninklijk Nederlands Meteorologisch Instituut). Hersbach (1996, pers. comm.) mentioned that there are good experiences with this kind of boundary condition for the North Sea. The third, and by far the most expensive, option is to perform a global or almost global (e.g. Atlantic) stand-alone run with the wave model for the whole period forced by coarse-resolution global winds. This may be important in cases in which swell might be present.

Lateral boundaries for PCM-HAMSOM. There is still much of ongoing discussion among ocean modellers about lateral boundary conditions for limited-area ocean models. We adopted a simple strategy suggested by Maier-Reimer (pers. comm., 1996) to provide ocean boundaries. We chose a model area larger than the one we are finally interested in and which we want to couple to the other modules. In this area the ocean is initialized by salinities and temperatures from Levitus (1982). The area includes a realistic bathymetry, but is closed at the boundaries. To avoid reflection, a very strong restoring to the Levitus salinities and temperatures at the two grid points closest to the boundary walls is preformed. This kind of boundary condition provides a quite reasonable circulation some grid points away from the walls (not shown). The extra relaxation area was chosen so that the effects of boundaries are negligible in the coupling area. We recommend an ocean model spin-up of a few months to dampen out initial oscillations due to the inconsistency between the density (temperature and salinity) field and the zero velocities at initialization.

The solution proposed above cannot be applied directly when tides should be included. Tides are introduced in PCM-HAMSOM by prescribing the sea surface elevation due to tides at the lateral boundaries. Since this is not possible when we have a closed basin, the strategy was modified slightly. First an ocean model spin-up with closed boundaries and an extra relaxation zone is performed. This run does not include tides. Sea surface elevation, temperature, and salinity of this run are stored and then provided as boundary conditions to the coupled run. For the coupled run we use an ocean area with open boundaries nested into the spin-up area. Here

tides are introduced as usually. A zero gradient boundary condition for the fluxes is applied at the open boundaries.

Exchange of information at the model interface. Transfer of information has been made safe by keeping the interface among the modules as small as possible. The basic concept is that a module writes its essential information to the coupling module as soon as it was calculated. Information is stored, and if necessary physically transformed and rescaled within the coupling module. If the modules ocean, waves or atmosphere need information from each other, it is obtained by a simple call to the coupling module.

The time steps of the modules might vary considerably. It may, for instance, be necessary to integrate the atmosphere module with two or five minute time steps, whereas the ocean could be integrated with a 20 minute time step or more. It is not necessary to decrease the ocean time step to the atmospheric one. The coupling module accumulates and averages the output of N uncoupled atmosphere time steps which in turn is later received by the ocean and the wave modules. There are no constraints for the ratio of the module time steps, except that

$$\Delta t_{atmosphere} \leq \Delta t_{waves} \leq \Delta t_{ocean} \tag{31}$$

Principally coupling takes place if

$$N_a \Delta t_{atmosphere} = N_w \Delta t_{waves} = N_o \Delta t_{ocean} \tag{32}$$

where Δt_x is the time step of the module x (atmosphere, waves, ocean), and N_a, N_w, and N_o are the smallest positive integer numbers possible. Usually, one might choose

$$\Delta t_{ocean} = N \Delta t_{waves} \tag{33}$$

with

$$\Delta t_{waves} = M \Delta t_{atmosphere} \tag{34}$$

Here coupling takes place every MN atmospheric time step.

4. The North Sea February 1993 storm

4.1. Model set-up and spin-up

To perform first experiments and test runs the model was set-up for the North Sea and the North East Atlantic (Figure 2). The horizontal resolution is roughly 18x18 km for the North

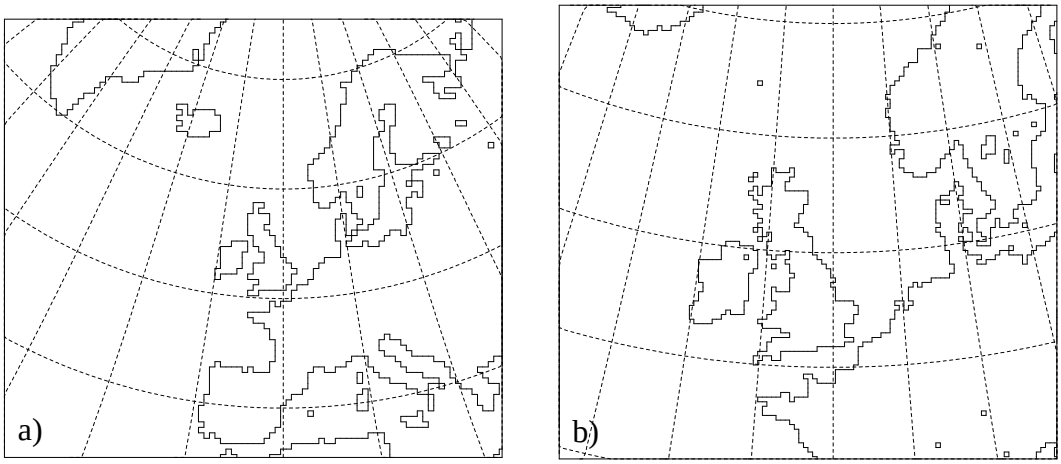

Figure 2: Land sea masks used in ECAWOM for the North East Atlantic (a), and the North Sea (b).

Sea and 50x50 km for the North East Atlantic. The time steps vary between 2 minutes for the atmosphere for the North Sea area and 20 minutes for the ocean for the North East Atlantic (Table 1).

Table 1: Model areas

Region	Abbreviation	Approximate horizontal resolution	Time steps atmosphere/waves/ ocean
North East Atlantic	KNM	50 x 50 km	5/20/20 min
North Sea	NOS	18 x 18 km	2/12/12 min

We forced the stand alone-ocean module with 6 hourly wind stresses, sea surface temperatures, and sea level pressure as provided by ECMWF for roughly three month to allow the baroclinic structure of the ocean model to adopt to the initial conditions. Because of missing sub-surface temperatures and salinities this was also the best way to adopt the ocean module to a quasi realistic state. At the end of the ocean spin-up we switched to the full coupled model and restarted the ocean from the final state achieved during the spin-up. The coupled ECA-WOM was integrated from February, 15th until March, 15th 1993. For the coupled simulation

we used the boundary data from the ECMWF analysis archive for the atmosphere, the artificial fetch condition for the waves (Section 3), and the results of the spin-up for the ocean. Climate files were generated according to the description in Section 3.

4.2. Synoptic situation

A series of storms moved over the North Sea in February 1993. Prior to the development of these storm systems, a calm high pressure situation was observed over Europe. The frontal zone was located over the North East Atlantic (DWD, 1993). The situation started to change towards more stormy weather on February 15th. The track of the cyclones was located over the North Sea and was oriented in a west-east direction at first, thereafter tilting to the north-west-southeast. Along this track a strong cyclone was moving with intensification over the North Sea, on February 21st. Within this storm the observed wind speed exceeded more than 25 m/s and the significant wave height reached a maximum nearby 10 m at the wave buoy NOC (Figure 7, 8). The waves were moving nearby southward with a period of roughly 12 s corresponding to a mean wave length of 250 m and a phase velocity of roughly 20 m/s (not shown).

4.3. Results

4.3.1. Atmosphere.

The atmospheric situation was hindcast quite reasonably by ECAWOM (Figure 3-6). A high pressure system is located west of the British Isles, and strong northwesterly winds can be found over the entire North Sea region. From the sea level pressure it can be inferred that the centre of the depression moved southeastward from the Norwegian Coast to the Southern Baltic Sea within 18 hours. The location of the cold front can be inferred from the strong humidity gradients at the 700 hPa geopotential surface. It was moving southwestward over the North Sea region and reached the German coast around 00 UTC on February, 21st. We compared these results with daily weather charts published by the German National Weather Service (DWD, 1993), and found a good agreement between the observed and the hindcast atmospheric situation. This is further supported by the comparison of the wind speed measured at 10 metres height at five buoys located in the North Sea with the ECAWOM results (Figure 8). The locations of these buoys can be inferred from Figure 9.

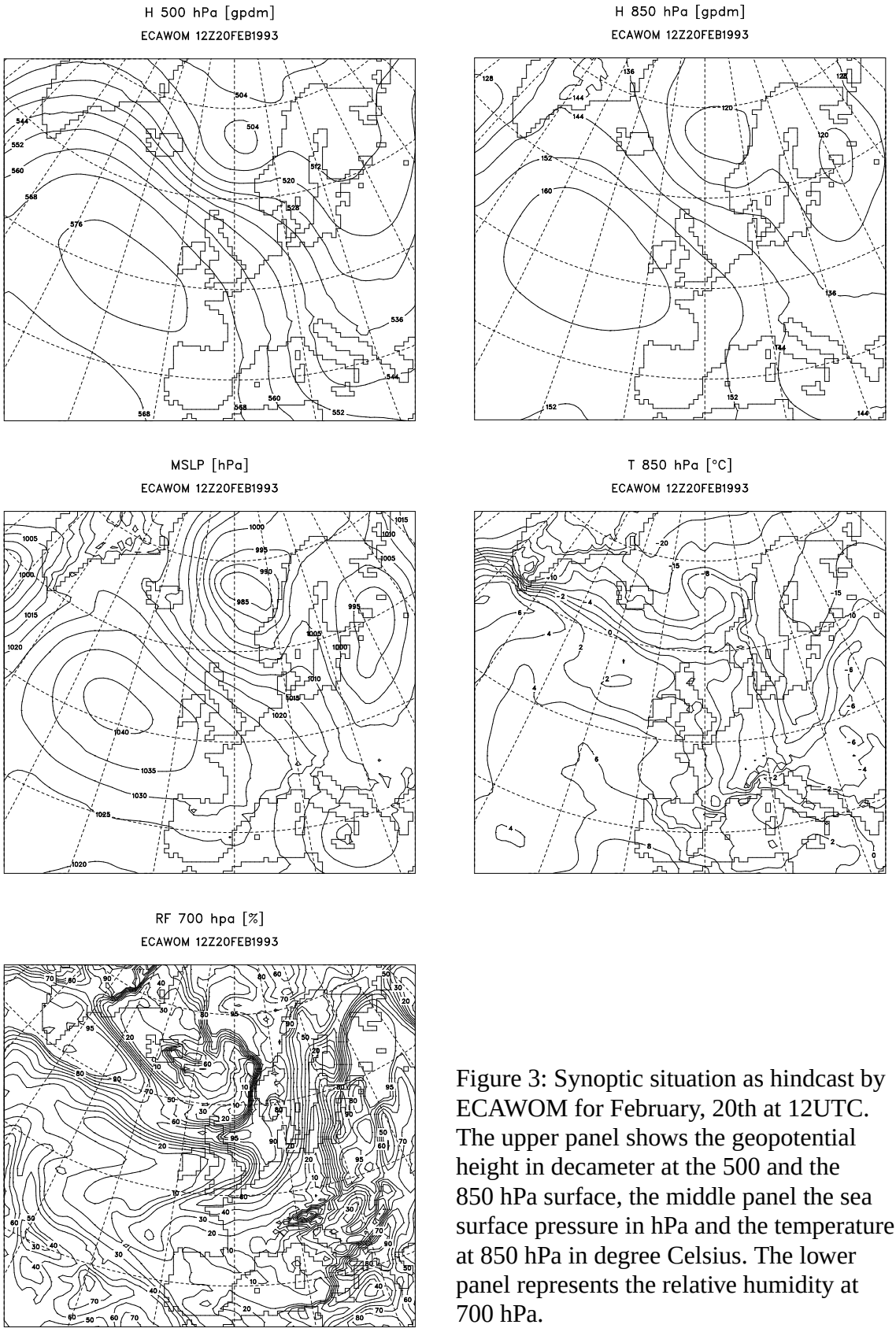

Figure 3: Synoptic situation as hindcast by ECAWOM for February, 20th at 12UTC. The upper panel shows the geopotential height in decameter at the 500 and the 850 hPa surface, the middle panel the sea surface pressure in hPa and the temperature at 850 hPa in degree Celsius. The lower panel represents the relative humidity at 700 hPa.

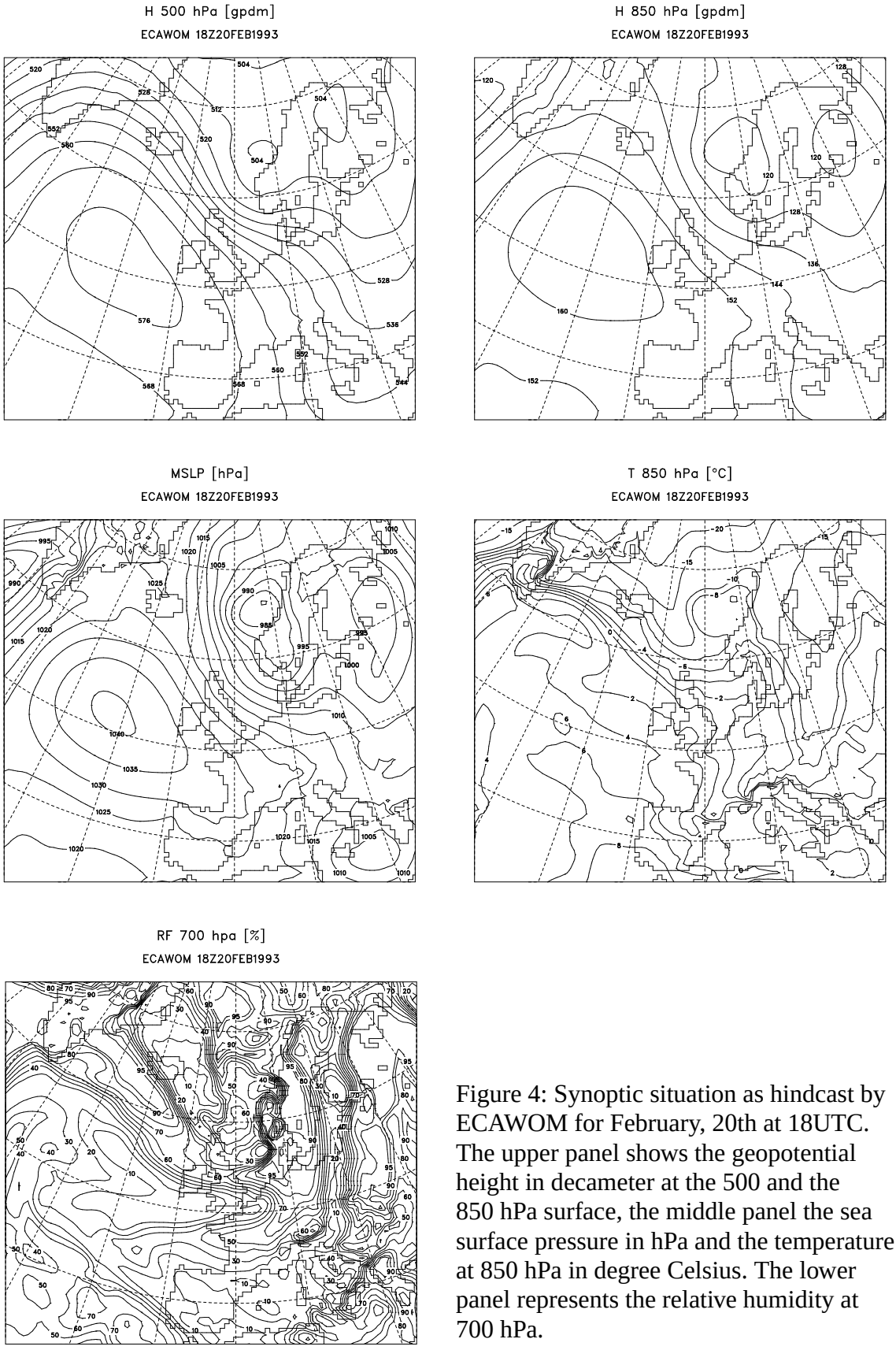

Figure 4: Synoptic situation as hindcast by ECAWOM for February, 20th at 18UTC. The upper panel shows the geopotential height in decameter at the 500 and the 850 hPa surface, the middle panel the sea surface pressure in hPa and the temperature at 850 hPa in degree Celsius. The lower panel represents the relative humidity at 700 hPa.

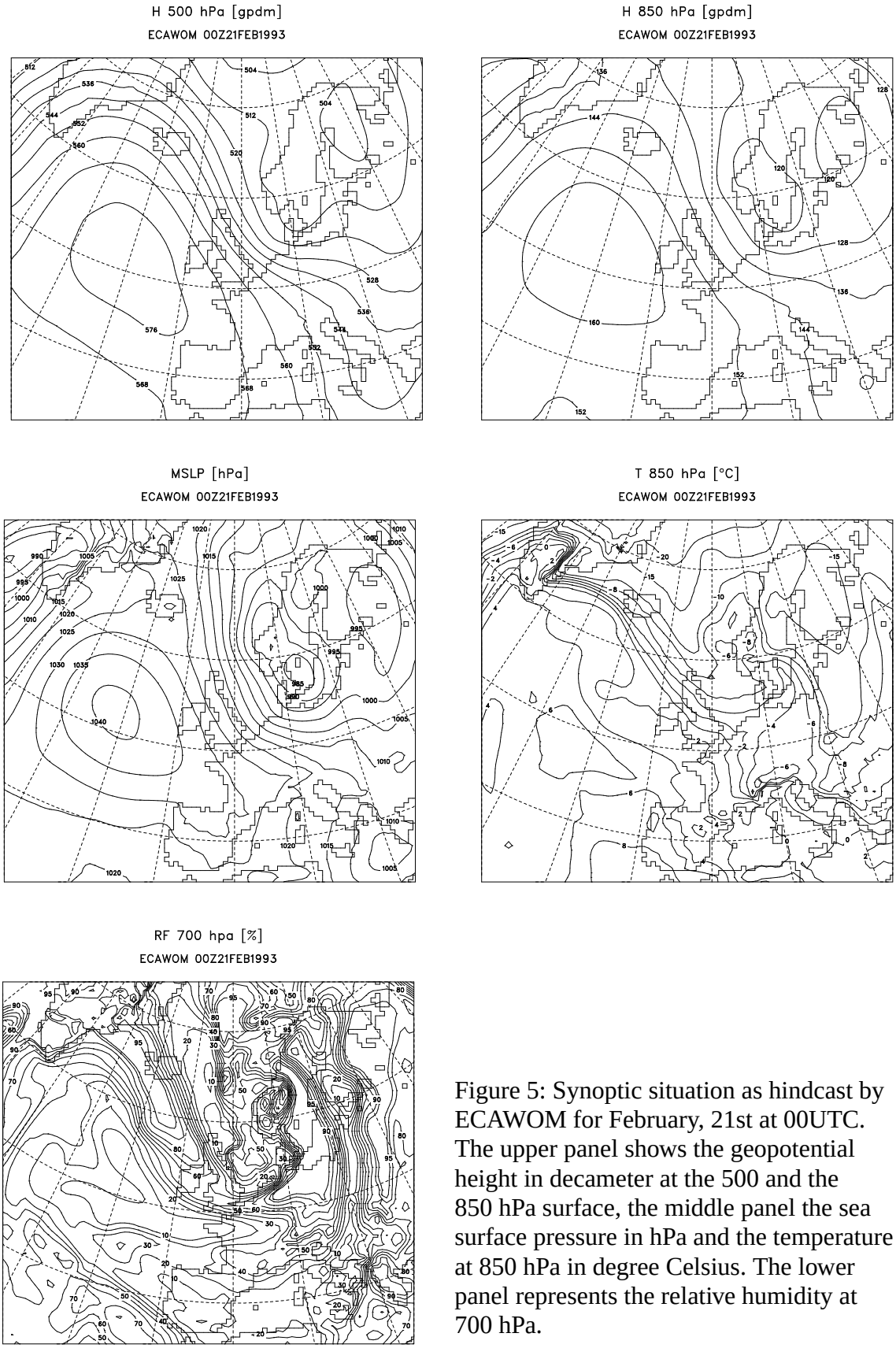

Figure 5: Synoptic situation as hindcast by ECAWOM for February, 21st at 00UTC. The upper panel shows the geopotential height in decameter at the 500 and the 850 hPa surface, the middle panel the sea surface pressure in hPa and the temperature at 850 hPa in degree Celsius. The lower panel represents the relative humidity at 700 hPa.

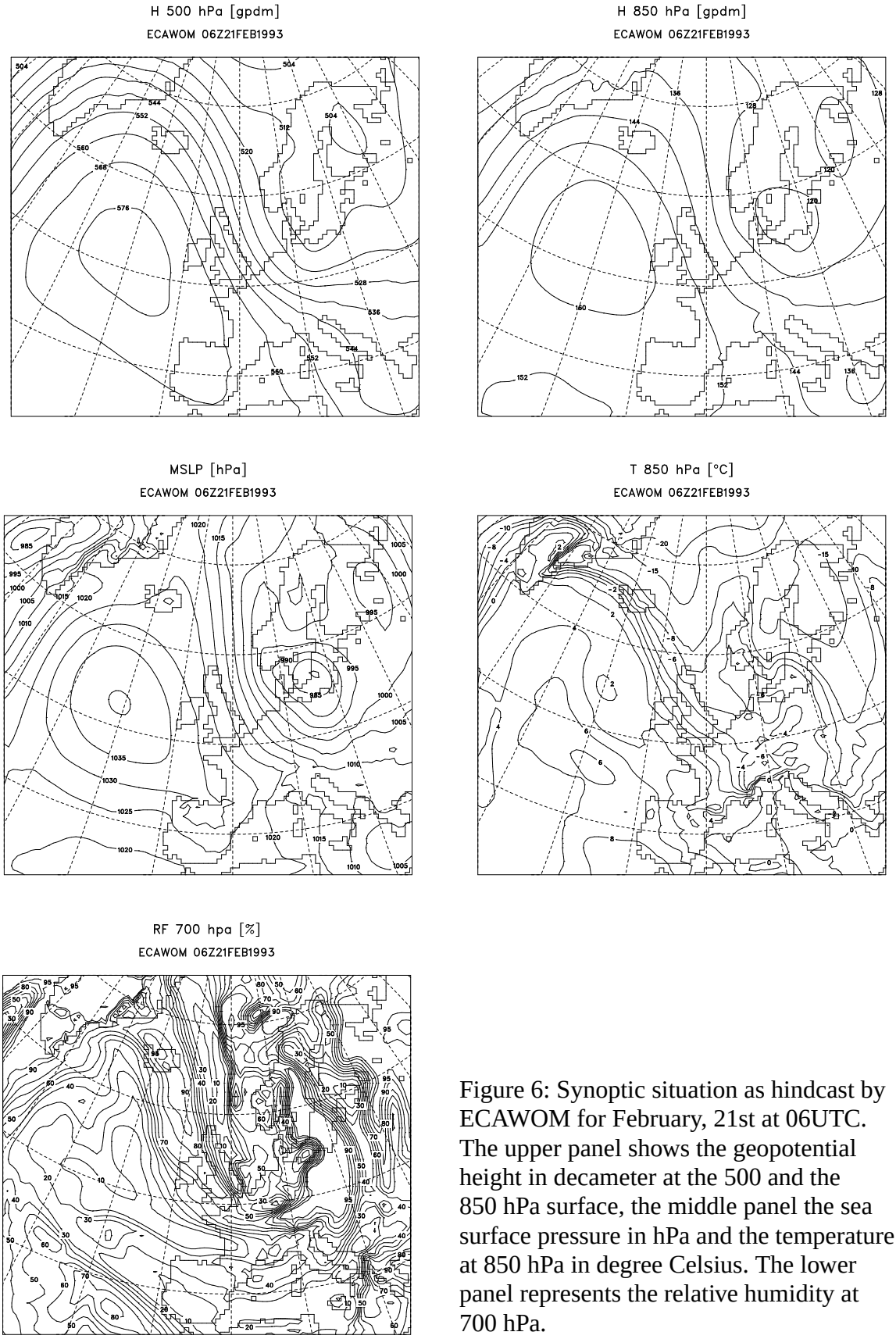

Figure 6: Synoptic situation as hindcast by ECAWOM for February, 21st at 06UTC. The upper panel shows the geopotential height in decameter at the 500 and the 850 hPa surface, the middle panel the sea surface pressure in hPa and the temperature at 850 hPa in degree Celsius. The lower panel represents the relative humidity at 700 hPa.

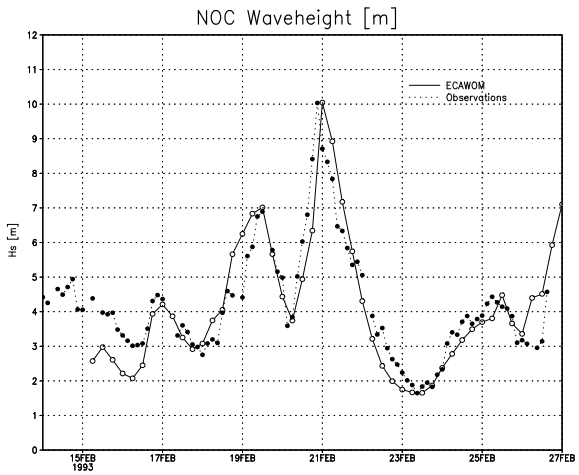

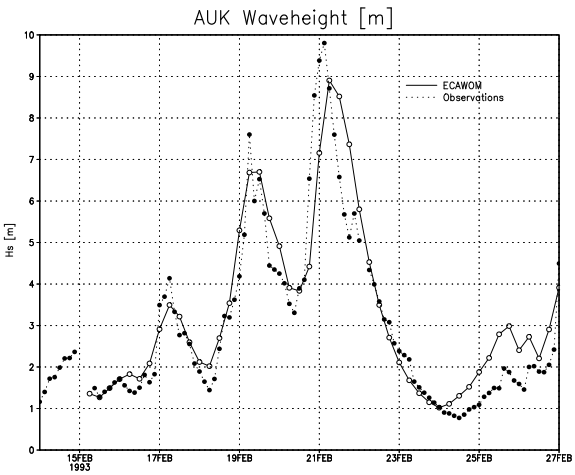

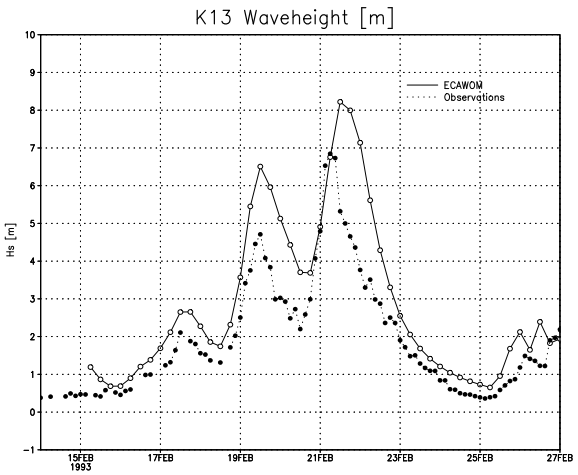

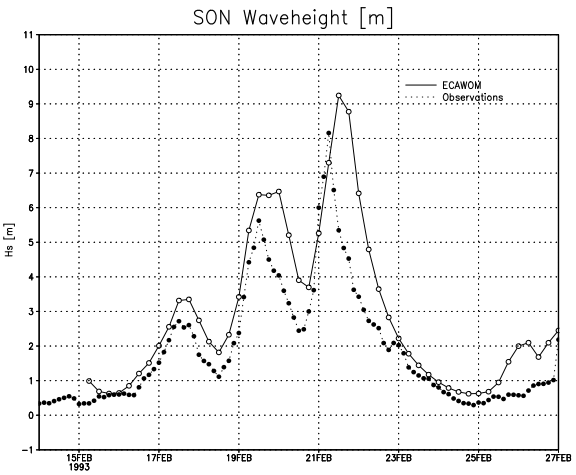

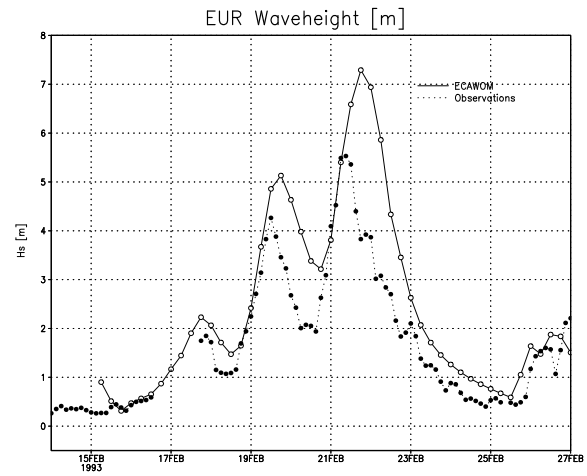

Figure 7: Significant wave height at 5 locations in the North Sea during the February 1993 storm as observed (dotted line) and hindcast by ECAWOM (solid line). The location of the buoys can be obtained from Figure 9

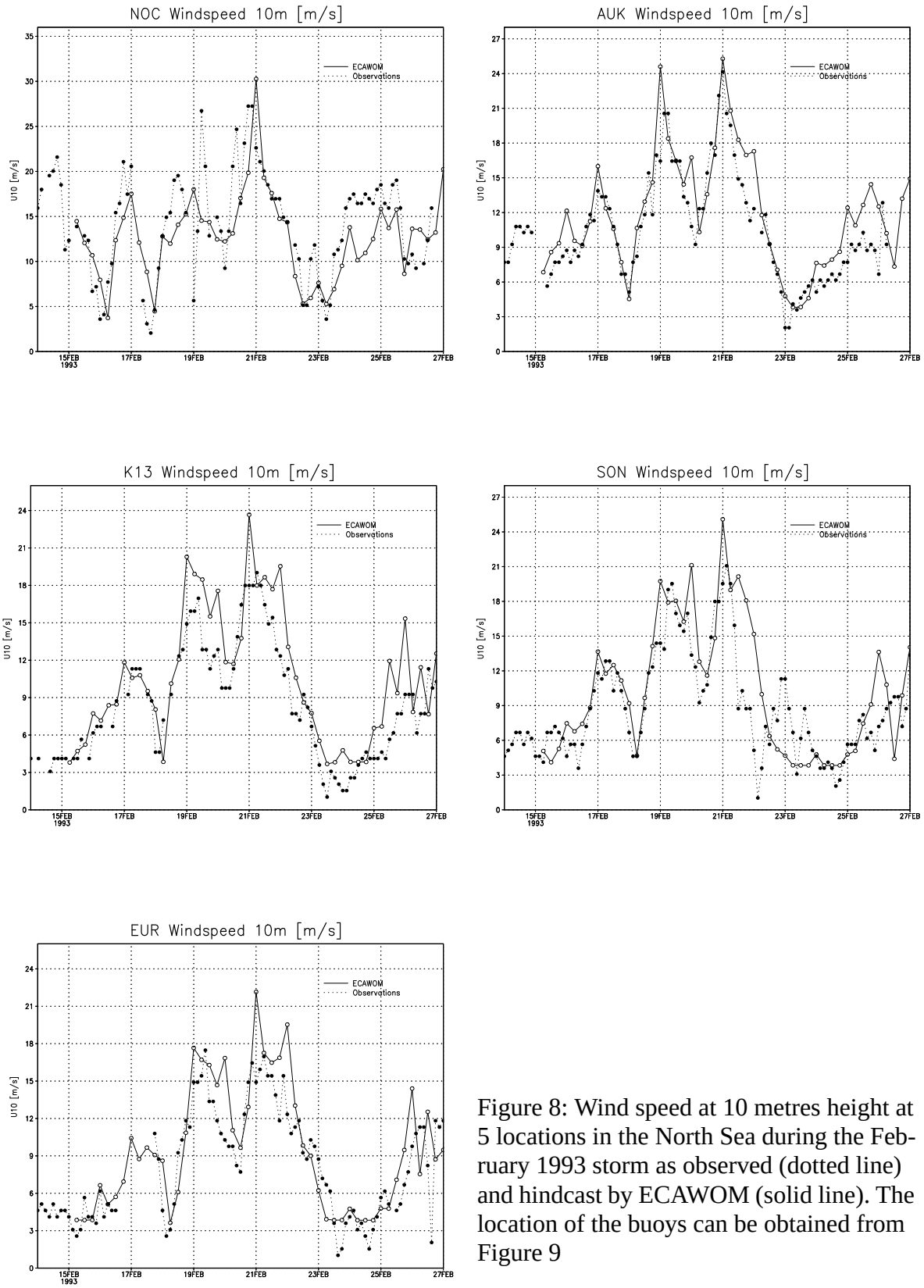

Figure 8: Wind speed at 10 metres height at 5 locations in the North Sea during the February 1993 storm as observed (dotted line) and hindcast by ECAWOM (solid line). The location of the buoys can be obtained from Figure 9

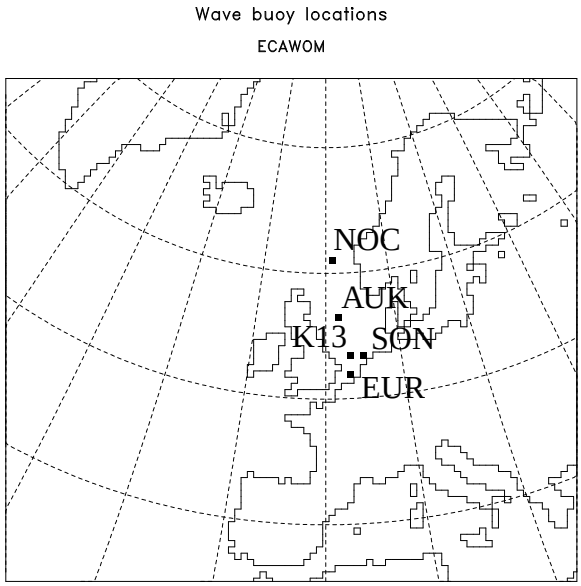

Figure 9: Locations of the wave buoys NOC, AUK, K13, SON, and EUR.

4.3.2. Waves

We compared the observed wave heights at station NOC, AUK, K13, SON, and EUR and with those computed by ECAWOM (Figure 7). There is a good agreement between the measured and the modelled data. The difference between observations and model results at the beginning of the time series is due to the fact that all WAM grid points were initialized with the same JONSWAP spectrum (Hasselmann et al., 1973), independent of the local winds at the initialization point. Thus, there is some time required to adopt the wave field to the local wind field. From Figure 7 it can be inferred that this adoption took almost two days for NOC. The observed wave heights at all other buoys were much closer to the JONSWAP spectrum, thus there is almost no initialization period.

The general time development of the wave height is to a good degree of approximation hindcast by ECAWOM. Especially at NOC, the agreement between observed and modelled wave heights is quite good. The model underestimates the wave height at AUK by roughly one meter around February 21st; however, it overestimates the wave height at K13, SON and EUR. The shape of the curve is reasonable for all buoys.

For the mean wave period a quite good agreement between the modelled and the observed data is again found, although single values may vary considerably (Figure 10). Again the initialization period is most obvious for NOC.

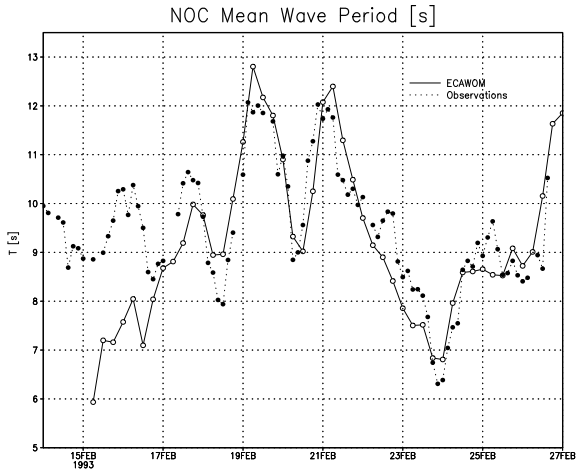

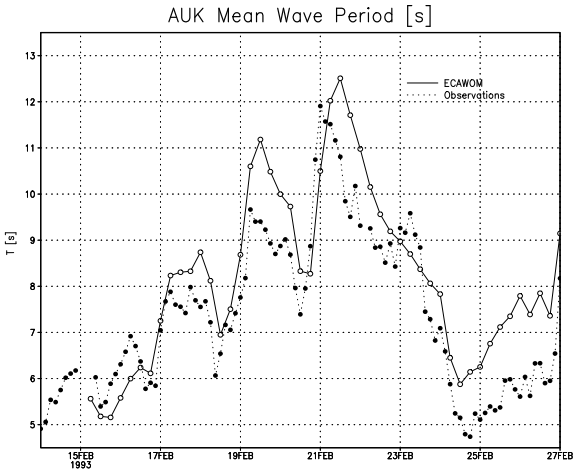

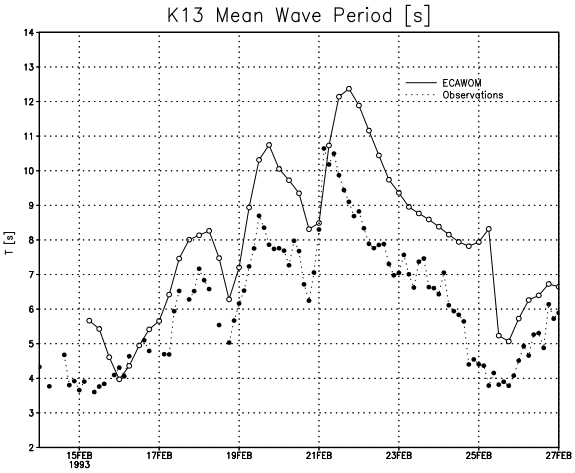

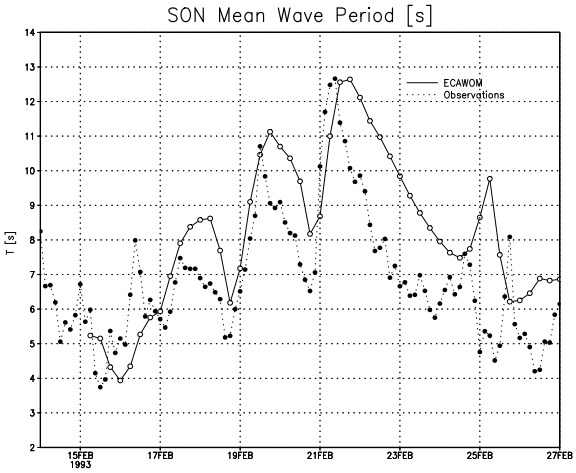

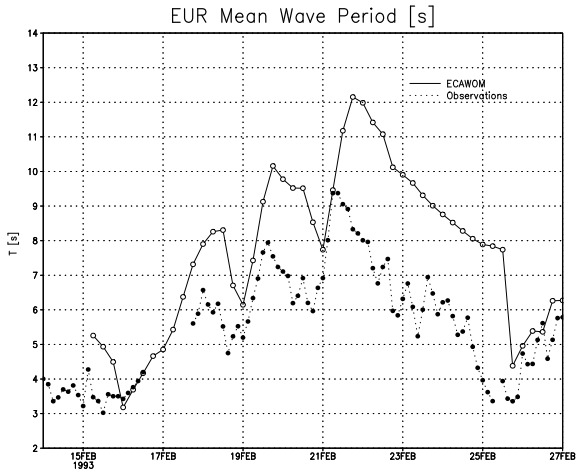

Figure 10: Mean wave period at 5 locations in the North Sea during the February 1993 storm as observed (dotted line) and hindcast by ECAWOM (solid line). The location of the buoys can be obtained from Figure 9.

At the peak of the storm at February 21st, 00 UTC, the maximum significant wave height is found northeast of Great Britain (Figure 11a). The highest waves do have periods of roughly 12 seconds, which corresponds to a wave length of roughly 250 meters and a group velocity of 20 m/s (Figure 11b). This is consistent with the results produced by the atmosphere module (Figure 5).

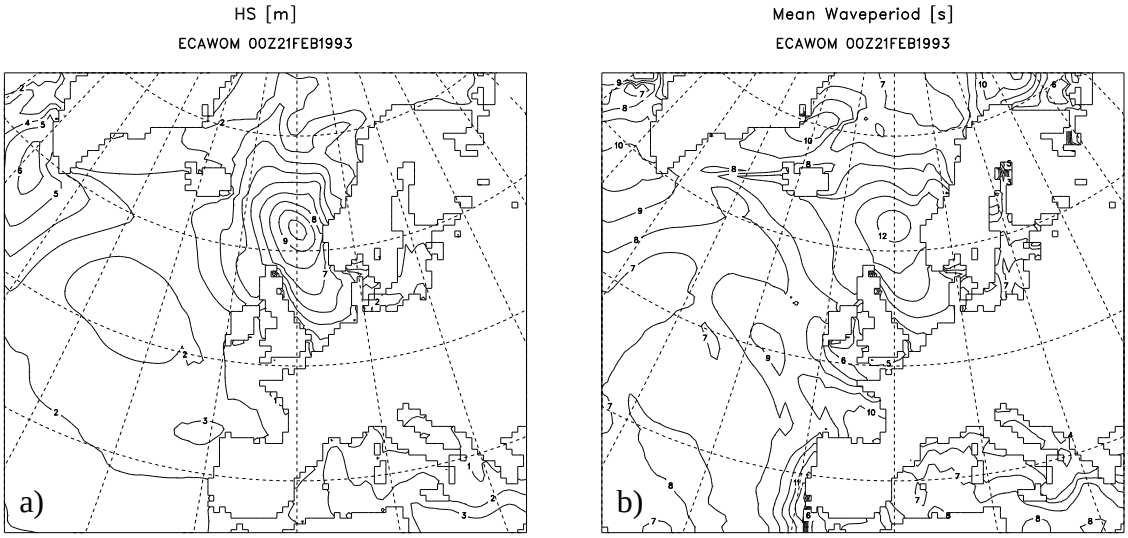

Figure 11: Significant wave height (a) and mean wave period (b) as hindcast by ECAWOM for February, 21st at 00UTC.

4.3.3. Ocean.

The surge at three locations along the British east coast can be seen in Figure 12. What immediately follows is that there is a general agreement between the observed and the hindcast values. At Sheerness the ECAWOM model underestimates the main peak by roughly 70 cm, whereas the previous peak is hindcast well, although with a longer duration. The general agreement between model and observations is less at Wick and Aberdeen. The surges at these tide gauges are, however, within the range of 20 to 60 centimetres compared to roughly 3 metres at Sheerness. Thus, the model seems to be able to reproduce relatively large surge at a reasonable level of agreement.

For Wick and Aberdeen there is a constant shift between the observations and the model results. Furthermore, both observed time series show a strong decrease between the end of January, and the begin of February, which could not be found in the time series of Sheerness (not shown). To check for possible reasons we re-ran the stand-alone ocean module forced with 6 hourly wind stresses, sea level pressure and sea surface temperatures from January 1st.

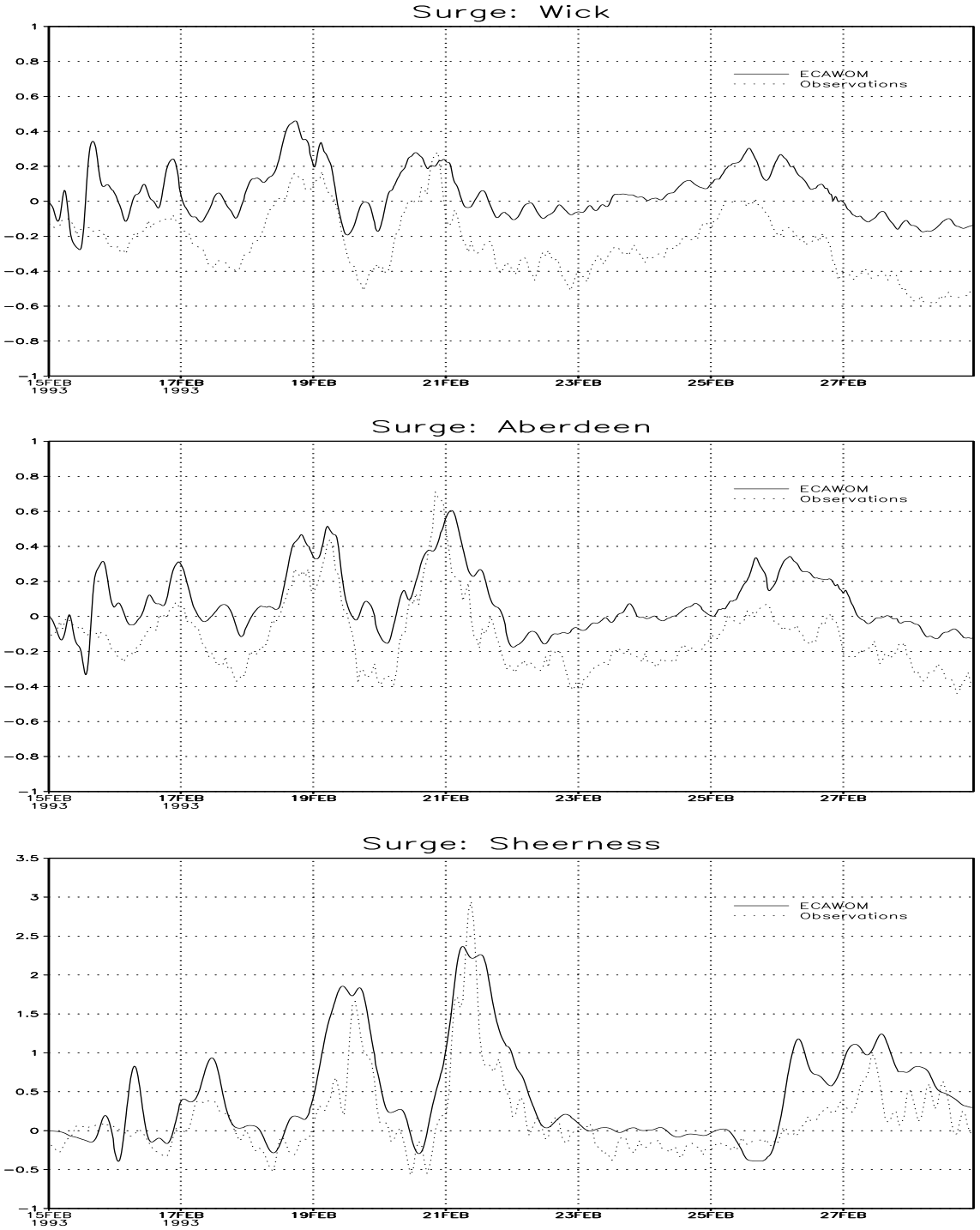

Figure 12: Sea surface elevation in meter at 3 tide gauges at the east coast of Great Britain as observed and as hindcast by ECAWOM.

However, the model failed to reproduce the strong decrease in the mean values at Wick and Aberdeen. So far, we could not determine whether there is something missing in the model, or if observations are disturbed. If we neglect the constant shift between observations and ECA-WOM results at Wick and Aberdeen, the agreement is reasonable.

The sequence Wick, Aberdeen, and Sheerness can be considered as a kind of north-south cross section along the British coast. We can thus interpret the phase shift between the maximum surge at the three tide gauges. From Figure 12 it can be inferred that the surge is propagating southwards. In the observations, the surge reaches Sheerness roughly 12 hours after passing Wick. In the model it took approximately 8 hours. At the Dutch and the Danish coast the surge is reasonably reproduced (not shown).

5. Summary

The European Coupled Atmosphere Wave Ocean model ECAWOM in its present set-up was introduced and described. The model is intend to fill the gap between global or nearly global large-scale and small-scale wave-ocean models and to provide consistent data sets simultaneously for the atmosphere, the waves and the ocean which may be used directly as boundary conditions for small-scale models. Coupling processes between the atmosphere, the waves and the ocean included in the model were reviewed and discussed.

To test the present model configuration initial experiments were carried out. The model was set-up for the North Sea and integrated for the 1 month period of February 1993. Preliminary analysis of the results suggest that the model is capable of reproducing the basic features of the atmospheric, the wave, and the surge characteristics for this 1 month period. The experiments are, however, relatively short and devoted to a single stormy period characterized by certain meteorological and wave conditions. Thus, only limited conclusions can be drawn, especially, as the quality of the results may vary as the meteorological and wave conditions change. A number of sensitivity experiments is necessary to systematically investigate the performance of the model for storms with different characteristics. For instance, a rapidly moving cyclone may be associated with relatively young waves, whereas under a slowly moving depression the waves may become fully developed under high wind conditions. A chain of depressions which will not allow the winds to drop under a certain windspeed will result in surge that may last for several days (e.g. February, 1990). The quality of ECAWOM hindcasts may vary under all these conditions. A systematic analysis of such cases may provide further inside into the

important coupling mechanisms and help to assess the quality of the model more precisely.

Another important topic which can not be assessed so far is the skill of the model for longer integrations (years or longer). We argue, however, that for long-term integrations important processes, as for instance the coupling of fresh water fluxes, are missing or lacking in the model. To identify those first order processes which have to be included or modified to bring the model into a good shape for long-term integrations a one year integration of the model in its present set-up is planned. This also helps to assess such important features as the reproduction of the annual cycle or a possible model drift.

To evaluate the potential of ECAWOM to provide boundary conditions for small scale high-resolution coastal wave-surge models Flather (1996, pers. comm.) forced the 2-d operational surge model of the Proudman Oceanographic Laboratory (POL) (Flather et al., 1991) with the meteorological forcing derived from ECAWOM and the atmosphere model of the UK Meteorological Office (UKMO). He found that surges with ECAWOM input were only about half of those with UKMO winds which agree with the observations. However, surges hindcast by ECAWOM itself were not that bad (Figure 12). One explanation, among others, is that the POL storm surge model is intended for use with UKMO boundary conditions. The winds are provided at the lowest model level, for which a general terrain-following coordinate may vary considerably in height, but is generally higher than 10 metres. On the other hand ECAWOM winds have been provided at 10 metres height and were generally less than the UKMO winds, thus leading to a considerable underestimation of the storm surges. Flather scaled up the ECAWOM winds by a factor of 1.2 and repeated the experiments. The storm surge hindcast by ECAWOM was improved significantly. To fully evaluate this problem, it is planned to repeat the run with the ECAWOM hindcast wind stresses instead of wind speeds and direction.

Acknowledgments

The authors gratefully acknowledge the help of Ernst Maier-Reimer who, with his experience in ocean modelling, contributed significantly to the fast and proper implementation of the ocean model. Michael Botzets knowledge and patience helped to become familiar with the HIRLAM and HIRHAM system and to track down all HIRLAM related problems quickly. We thank Ole Bossing Christensen for the fast job in providing several hundred megabytes of boundary data for the test experiments. We also thank Hans Hersbach for fixing a bug in the wave model. He also brought to our attention easy-to-use boundary conditions for WAM and provided the buoy data for the North Sea. Roger Flather kindly provided the british tide gauge data and performed the experiments with the high resolution wave-ocean model forced with ECAWOM winds. We acknowledge the help of Scott Hanson for carefully reading this manuscript. Last but not least we gratefully thank Hans von Storch whose interactive skills saved us from going down in the sometimes rough seas of the project. The work was carried out with support from the Commissions of the European Community (contract MAS2CT940091).

References

Alvarez, E.F., 1995: Modelado numerico de la circulacion estuarica en la ria de vigo, Programa de Clima Marítimo, Madrid, 64pp.

Arakawa, A., and V.R. Lamb, 1977: Computational design of the basic dynamic processes of the UCLA general circulation model. Methods Comput. Phys., 17, 173-265.

Backhaus, J.O., 1983: A semi-implicit scheme for the shallow water equations for applications to shelf sea modelling. Continental Shelf Research, 2, 243-254.

Backhaus, J.O., 1985: A three-dimensional model for the simulation of shelf sea dynamics. Deut. Hydrogr. Zeitschr., 38, 165-187.

Burgers, G., 1990: A guide to the NEDWAM wave model. KNMI Scientific Report WR-90-04, 81pp.

Chalikov, D., and V.M. Makin: 1991: Models of the wave boundary layer. Boundary Layer Meteorol., 63, 65-96.

Charnock, H., 1955: Wind stress on a water surface. Q.J.R. Meteorol. Soc., 81, 639-640.

Christensen, J.H., and E. Maijgaard, 1992: On the construction of a regional atmospheric climate model. Danish Meteorological Institute, Technical Report 92-14, 21pp.

DKRZ Modelling Group, 1993: The ECHAM3 atmospheric general circulation model. DKRZ Technical report No. 6, Hamburg, September 1993, 184pp.

DWD, 1993: Wetterkarte, Amtsblatt des Deutschen Wetterdienstes, Deutscher Wetterdienst, Offenbach, 1993.

Flather, R.A., R. Protocor, and J. Wolf, 1991: Oceanographic forecast models. pp.15-30, in Computer modelling in the environmental sciences, (ed.D.G.Farmer and M.J.Rycroft). Oxford: Clarendon Press. 379pp.

Giorgi, F., L.O. Mearns, 1991: Approaches to the simulation of regional climate change. A review. Rev. Geophys., 29, 191-216

Günther, H., S. Hasselmann, and P.A.E.M. Janssen, 1992: Wamodel cycle4, revised. DKRZ Technical report No. 4, Hamburg, October 1992, 102pp.

Hasselmann, K., T.P. Barnett, E. Bouws, H. Carlson, D.E. Cartwright, K. Enke, J. A. Ewing, H. Gienapp, D.E. Hasselmann, P. Krusemann, A. Meerburg, P. Müller, D.J. Olbers, K. Richter, W. Sell, and H. Walden, 1973: Measurements of wind wave growth and swell decay during the Joint North Sea Wave project JONSWAP. Dtsch. Hydrogr. Zeitschr. Suppl. A 8, 12, 95pp.

Huang, D., 1995: Modelling studies of barotropic and baroclinic dynamics in the Bohai Sea. Ber. Zentr. Meeresforsch., B, 17, Institut für Meereskunde, Hamburg, 1995, 126pp.

Janssen, P.A.E.M., 1989: Wave induced stress and the drag of air flow over sea waves. J. Phys. Oceanogr., 19, 745-754.

Janssen, P.A.E.M., 1991: Quasi-linear theory of wind wave generation applied to wave forecasting. J. Phys. Oceanogr., 21, 1631-1642

Janssen, P.A.E.M, and P. Viterbo, 1996: Ocean waves and the atmospheric climate. J. Clim., 9, 1296-1287.

Kållberg, P., and R. Gibson, 1977: Lateral boundary conditions for a limited area version of the ECMWF model. WGNE Progress report No. 14, WMO Geneva.

Källén, E. (ed), 1996: HIRLAM documentation manual, system 2.5.

Komen, G.J., L. Cavaleri, M. Donelean, K. Hasselmann, S. Hasselmann, P.A.E.M. Janssen, 1994: Dynamics and modelling of ocean waves, Cambridge, 1994, 532pp.

Large, W.G., and S. Pond, 1982: Sensible and latent heat flux measurements over the ocean. J. Phys. Oceanogr., 12, 464-482.

Levitus, S., 1982: Climatological atlas of the world ocean. NOAA Prof. Pap., 13, U.S. Govt. Print. Office, Washington, D.C.

Louis, J.F., 1979: A parametric model of vertical eddy fluxes in the atmosphere. Boundary Layer Meteorol., 17, 187-202.

Louis, J.F., M. Tiedtke, and J.F. Geleyn, 1982: A short history of the PBL parameterization at ECMWF. Proceedings, ECMWF workshop on planetary boundary layer parameterization, Reading, 25-27 Nov. 81, 59-80.

Makin, V.K., V.N. Kudryavtsev, and C. Mastenbroek, 1995: Drag of the sea surface. Boundary Layer Meteorol, 73, 159-182.

Makin, V.K., 1996: Parametrization of sensible heat and moisture fluxes. Draft for the ECA-WOM meeting in Venice, February 26, 1996.

Mastenbroek, C., and S. Christopoulos, 1995: Review of coupling processes between waves and ocean, draft.

Miles, J.W., 1957: On the generation of surface waves by shear flow. J. Fluid Mech., 3, 185.

Pond, S., G.T. Phelps, J.E. Paquin, G. McBean, and R.W. Stewart, 1971: Measurements of the turbulent fluxes of momentum, moisture, and sensible heat over the ocean. J. Atmos. Sci., 28, 901-917.

Rodriguez I., 1996: Modelado de procesos barotrÆpicos y baroclÕnicos en la costa Noroeste de Africa. PhD thesis, Las Palmas University, 222 p.

Simmons, A.J., and D.M. Burridge, 1981: An energy and angular-momentum conserving vertical finite difference scheme and hybrid coordinates. Mon. Wea. Rev., 109, 758-766.

Smith, S.D., 1980: Wind stress and heat flux over the ocean in gale force winds. J. Phys. Oceanogr., 10, 709-726.

Smith, S.D., 1988: Coefficients for sea surface wind stress, heat flux and wind profiles as a function of wind speed and temperature. J. Geophys. Res., 93, C12, 15467-15472.

Snyder, R.L., F.W. Dobson, J.A. Elliot, and R.B. Long, 1981: Array measurements of atmospheric pressure fluctuations above surface gravity waves. J. Fluid. Mech., 102, 1-59.

UNESCO, 1983: Algorithms for computation of fundamental properties of sea water. UNESCO Technical Papers in Marine Sci., 44, Paris.

WAMDI Group, 1988: The WAM model - a third generation ocean wave prediction model. J. Phys. Oceanogr., 18, 1775-1810.

von Storch, H., 1995: Inconsistencies at the interface of climate impact studies and global climate research. Meteorol. Zeitschr., 4, 72-80.

Weber, S., 1994: Statistics of the air-sea fluxes of momentum and mechanical energy in a coupled wave-atmosphere model. J. Phys. Oceanogr., 24, 1388-1398.

Wolf, J., K.P. Hubbert, and R.A. Flather, 1988: A feasibility study for the development of a joint surge and wave model. Report No.1 of the Proudman Oceanographic Laboratory, Birkenhead, United Kingdom, 109pp.